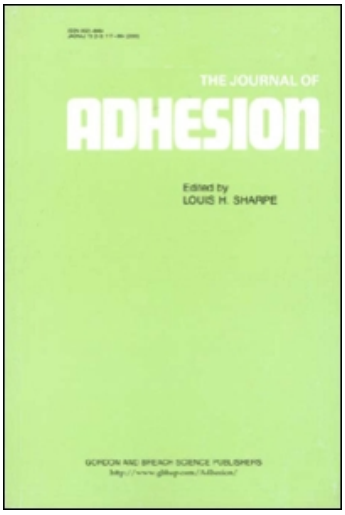

The Journal of Adhesion
Publication details, including instructions for authors and subscription information:
http://www.informaworld.com/smpp/title~content=t713453635

Non-Destructive In Situ Analysis of Interface Processes and Thin Film Growth

M. Buck[a]; Ch. Dressler[a]; M. Grunze[a]; F. Träger[b]
[a] Institut für Angewandte Physikalische Chemie, Heidelberg, Germany [b] Fachbereich Physik der Universität Kassel, Kassel, Germany

To cite this Article Buck, M. , Dressler, Ch. , Grunze, M. and Träger, F.(1996) 'Non-Destructive In Situ Analysis of Interface Processes and Thin Film Growth', The Journal of Adhesion, 58: 3, 227 — 241
To link to this Article: DOI: 10.1080/00218469608015202
URL: http://dx.doi.org/10.1080/00218469608015202

J. Adhesion, 1996, Vol. 58, pp. 227–241
Reprints available directly from the publisher
Photocopying permitted by license only

Non-Destructive In Situ Analysis of Interface Processes and Thin Film Growth*

M. BUCK**, CH. DRESSLER and M. GRUNZE

Institut für Angewandte Physikalische Chemie, Im Neuenheimer Feld 253, 69120 Heidelberg, Germany

F. TRÄGER

Fachbereich Physik der Universität Kassel, Heinrich-Plett Strasse 40, 34132 Kassel, Germany

(Received July 3, 1995; in final form October 5, 1995)

Optical second harmonic generation (SHG) was applied to monitor the growth of films of polyamic acid on polycrystalline gold substrates. Different diamines such as 4,4'-oxydianiline (ODA), 4,4'-diaminodiphenyl disulfide (DAPS) and 4,4'-diaminobiphenyl (benzidine) were codeposited from the gas phase with pyromellitic dianhydride (PMDA). Depending on the diamine, the second harmonic signal varies differently during formation of the polymer/metal interface and the subsequent film growth. A three-layer model which takes into account the optical properties of thin films reveals that the shape of the thickness-dependent SH signal is related to the orientation of the molecules in the film. A fit of the experimental data based on the model indicates a structural transition that occurs several tens of nanometers above the substrate for PMDA/ODA and PMDA/DAPS. The experiments demonstrate that SHG can be applied to monitor the growth of thin films and to extract structural information.

KEY WORDS: Film growth; polymer films; polymer-metal interfaces; polyamic acid; in situ monitoring; second harmonic generation.

I. INTRODUCTION

The need for non-destructive techniques which give access to interfaces of technical relevance, *e.g.* solid/liquid or solid/solid, has been the driving force for the development of first-order nonlinear optical techniques (NLO) such as second harmonic generation (SHG) and sum frequency generation (SFG) as analytical tools.[1–5] Both methods combine the advantages of optical techniques with an inherent sensitivity to interface characteristics in the case of centrosymmetric media. Moreover, the experimental simplicity is another aspect which has led to a widespread application of SHG for interface studies throughout the past decade. Having been applied mostly to examine the immediate interfacial region between two centrosymmetric media and to

* Presented at EURADH94, Mulhouse, France, September 12–15, 1994, a conference organized by the Section Française de l'Adhesion, division de la Société Française du Vide.

** Corresponding author.

characterise Langmuir-Blodgett films,[6] second harmonic generation has been extended more recently to monitor the growth of thin inorganic[7–10] and organic films.[11,12]

In the experiments presented below, the growth of films of polyamic acid (PACS) was monitored *in situ* and in real time with second harmonic generation. In contrast to the technical process of spin coating, the films are deposited from the gas phase by evaporation of the monomer constituents from two Knudsen cells.[13] Polyamic acid is the precursor polymer of polyimide (PI), a polymer widely used for industrial applications, *e.g.* in microelectronic components.[14] The reaction scheme is depicted in Figure 1. PACS(III) is formed at room temperature by reaction of a dianhydride (I) with a diamine (II). Curing of the PACS film at temperatures of about 450 K yields the polyimide (IV).

The present paper is organised as follows. In Section II a brief introduction to second harmonic generation at interfaces and in thin films is given. A three-layer model is introduced and the basic elements necessary for the understanding of the experimental

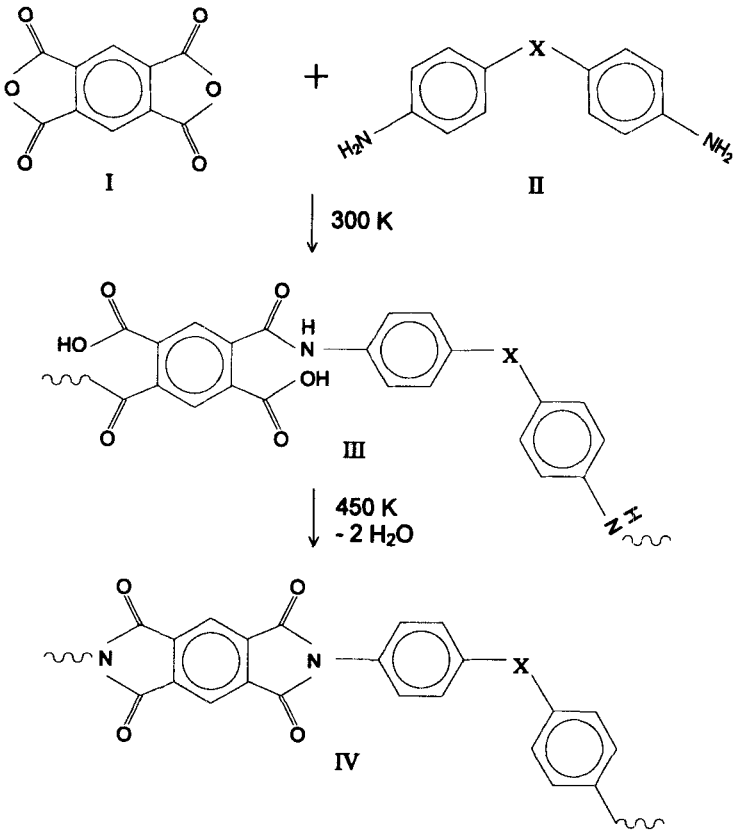

FIGURE 1 Reaction scheme of the formation of polyimide IV. As an intermediate step polyamic acid III (PACS) is formed at room temperature from a dianhydride I (pyromellitic dianhydride, PMDA) and a diamine (X = O: 4,4'-oxydianiline (ODA), X = S-S: 4,4'-diaminodiphenyl disulfide, no X: benzidine). At elevated temperatures the condensation reaction to polyimide takes place.

results are discussed. After the experimental details (Sec. III), the results are presented (Sec. IV) and discussed (Sec. V) on the basis of the model outlined in the theoretical part.

II. THEORY

The expressions given below are based on the electric dipole approximation. For details, the reader is referred to the literature.[1,15]

In matter an intense electric field $E(\omega)$, *e.g.* of a laser, induces a polarisation

$$\boldsymbol{P} = \chi^{(1)}\boldsymbol{E}(\omega) + \chi^{(2)}\boldsymbol{E}(\omega)\boldsymbol{E}(\omega) + \chi^{(3)}\boldsymbol{E}(\omega)\boldsymbol{E}(\omega)\boldsymbol{E}(\omega)\cdots \tag{1}$$

where $\chi^{(n)}$ denotes the linear and higher order nonlinear susceptibilities which are tensors of rank $n+1$. The first nonlinear term is the source of the second harmonic signal (SH). The SH intensity is given by

$$I_{\mathrm{SHG}} \propto |\boldsymbol{P}(2\omega)|^2 \tag{2}$$

with

$$\boldsymbol{P}(2\omega) = \sum_{ijk} \boldsymbol{e}_i \chi^{(2)}_{ijk} E_j(\omega) E_k(\omega) \tag{3}$$

In Equation (3) the polarisation is expressed as the sum of the different tensor elements of $\chi^{(2)}$. i, j, k represent the axes of a Cartesian coordinate system x, y, z. $\boldsymbol{e}_i$ denotes the unit vector along the direction i. E_j and E_k refer to the polarisation components of the incident fundamental field. In general, the susceptibility is a complex quantity, *i.e.* is characterised by its magnitude and its phase. Since only the nonlinear susceptibility of lowest order is considered in this paper we omit the superscript from now on.

For SHG, the susceptibility tensor generally consists of 18 independent elements. Fortunately, symmetry reduces this large number substantially. The layered systems considered in this paper are isotropic in the plane of the film and substrate. As a result of this azimuthal isotropy, only three independent elements, χ_{zzz}, $\chi_{zxx} = \chi_{zyy}$ and $\chi_{xzx} = \chi_{yzy}$, remain where z and x define the plane of incidence with x being parallel to the substrate. y is perpendicular to x and z (Fig. 2). As inferred from Equation (3) the number of tensor elements contributing to the total SHG signal depends on the polarisation of the incident fundamental field. If $\boldsymbol{E}(\omega)$ is polarised along the y-axis ($j = k = y$, s-polarisation) the only relevant tensor element is χ_{zyy}. Therefore, the polarisation has a z-component, only. In the case of $\boldsymbol{E}(\omega)$ being parallel to the plane of incidence (p-polarisation) all three tensor elements contribute and the total SH signal is a superposition of z- and x-polarised fields.

Based on symmetry arguments an SH signal vanishes in media with a center of inversion. An SH signal, however, can be generated at the interface between two such media, *i.e.* where the inversion symmetry is necessarily broken. Additional contributions from the bulk have to be taken into account if at least one of the media lacks inversion symmetry.

In the experiments presented here the growth of thin organic films on a polycrystalline metal substrate was examined. As illustrated by Figure 2, the samples represent

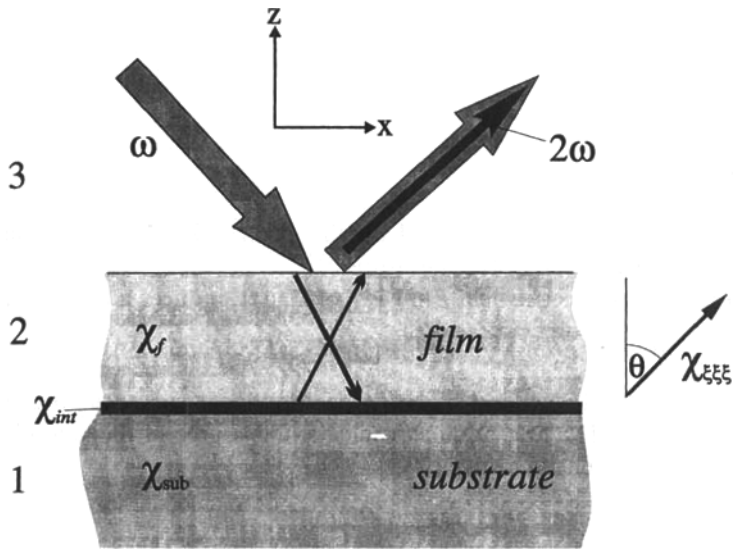

FIGURE 2 Scheme of second harmonic generation from a three-layer system. The SH signal is generated in the film and at the substrate/film interface. The corresponding macroscopic first order nonlinear susceptibilities are represented by χ_f and χ_{int}, respectively. The microscopic molecular susceptibility is characterised by $\chi_{\xi\xi\xi}$ tilted away from the surface normal by an angle θ. The up- and downward pointing arrows in the film symbolize multiple reflections both of the fundamental and harmonic waves.

three-layer systems consisting of an isotropic substrate (medium 1), the film (medium 2) and the surrounding medium (3) which is isotropic as well. As mentioned already, an SH signal can always be generated at the interfaces. In our case, only the contribution of the film/substrate interface is relevant. The nonlinear susceptibility of the film surface is negligibly small and can be omitted. If the film is anisotropic, *i.e.* non-centrosymmetric, a second contribution from the bulk of the film adds coherently to the interface signal. The total signal detected in medium 3 then is

$$I_{SHG} \propto |\boldsymbol{E}_{int}^{2\omega}(d, \chi_{int}) + \boldsymbol{E}_{f}^{2\omega}(d, \chi_f)|^2 \tag{4}$$

where $\boldsymbol{E}_{int}^{2\omega}$ represents the electric field of the harmonic wave originating from the interface and $\boldsymbol{E}_{f}^{2\omega}$ is the contribution of the film. d is the film thickness and χ_{int} and χ_f denote the susceptibility tensors which characterise the nonlinear optical properties of the interface and film, respectively. A brief qualitative description of the factors governing the total SH intensity is given here and we refer to the literature for a detailed quantitative treatment:[16,17] For the thickness dependence of the signal two points are essential. First, not only does the contribution of the film depend upon its thickness but also the signal originating from the interface. Therefore, even if the film did not have a measurable nonlinear susceptibility the detected SH signal would be thickness dependent. Secondly, the two contributions do not change in a simple way as a function of film thickness but display a rather complicated behavior. These two points are the consequence of multiple reflections of the light at the interfaces of the film. Upward and

downward propagating waves are generated causing interference. The thickness dependence of the interface signal is determined by the linear optical properties of the three-layer system and, therefore, is described by the optical properties of stratified media.[18] The contribution of the film is calculated from the inhomogeneous polarisation waves in the film and from the homogeneous waves in the film and in the adjacent media by meeting the boundary conditions at $z = 0$ and $z = d$. This leads to a set of linear equations from which the thickness dependence of the SH signal of the film can be calculated either analytically or numerically.[7,8,12,16,17]

After this qualitative discussion of the factors causing the thickness dependence of the SH signal we now turn to the susceptibilities and start with the interface susceptibility χ_{int}. It can be regarded as a sum of two terms given by:

$$\chi_{int} = \chi_{sub} + \chi_{sf} \tag{5}$$

where χ_{sub} is the susceptibility of the substrate without film and χ_{sf} denotes its alteration when the substrate/film interface is formed. Once the interface is formed after the initial stage of the deposition, χ_{int} remains constant and the contribution of the interface to the total SH signal varies as a function of the film thickness only because of linear optical effects.

The nonlinear susceptibility of the film, χ_f, allows one to extract information on the orientation of the molecules in the films by SHG. For this purpose, the macroscopically-determined susceptibility tensor, χ_f, which is defined in the coordinate system of the substrate, has to be related to the microscopic susceptibility of the NLO-active units in the film. A simple model connects the two quantities: local field effects are neglected and, furthermore, the microscopic susceptibility is assumed to have only a single nonvanishing tensor element, $\chi_{\xi\xi\xi}$, where ξ is an axis of a properly chosen coordinate system of the NLO-active unit in the film. The three tensor elements of χ_f are, thus, given by:

$$\chi_{zzz} \propto {}^1N\chi_{\xi\xi\xi}\langle\cos^3\theta\rangle \tag{6}$$

$$\chi_{xzx} = \chi_{zxx} \propto {}^1N\chi_{\xi\xi\xi}\langle\sin^2\theta\cos\theta\rangle \tag{7}$$

where θ is the tilt angle of the molecular susceptibility with respect to the surface normal, as illustrated in Figure 2, and ${}^1N$ is the density of the SH active molecules in the film. The brackets indicate an averaging over a distribution of tilt angles. As seen from Equations (6) and (7), the magnitudes of the tensor elements relative to each other are altered upon variation of the tilt angle, θ, of the molecular susceptibility. Since the amplitudes of the electric fields change differently as a function of distance from the substrate for the fundamental and harmonic waves and for different polarisations, the relative contributions of the three elements vary with the distance from the substrate as well. Consequently, the variation of the SH signal as a function of film thickness depends on the magnitudes of the tensor elements relative to each other. Solving the above mentioned set of equations under the assumption of this simple model permits one to extract orientational information from the thickness dependence of the SH signal. An impression of the sensitivity of the thickness-dependent SH signal to changes of the tilt angle, θ, is given by Figure 3. In this calculation, pp-polarisation is assumed, *i.e.* the polarisation of the incident fundamental and detected second harmonic beams

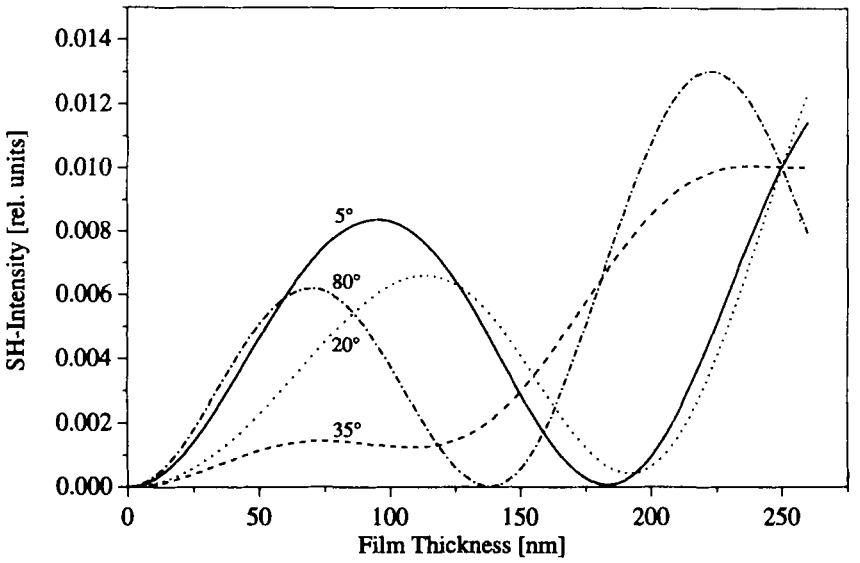

FIGURE 3 Thickness dependence of the SH intensity ($\lambda_{2\omega} = 532$ nm, pp-polarisation) of a film calculated for different inclination angles of $\chi_{\zeta\zeta\zeta}$. For the linear indexes of refraction the values of polyimide (film) and glass (substrate) are used. The angle of incidence of the fundamental beam is 45°. To allow better comparison the curves are scaled to the same value at a film thickness of 250 nm. The scaling factors are 1(5°), 1.8(20°), 0.86(35°), 3.1(80°).

are parallel to the plane of incidence. The fundamental wavelength and the angle of incidence were set to $\lambda = 1064$ nm and 45°, respectively. The inclination angle, θ, of the molecular unit was varied between 5° and 80°. The linear optical constants used in the calculation are representative for a polyimide film ($n_\omega = 1.72$, $n_{2\omega} = 1.80$)[19] on a glass substrate ($n_\omega = 1.50$, $n_{2\omega} = 1.51$)[20]. Other values, *i.e.* different film and substrate materials, yield shapes of the SH signal different from those shown in Figure 3. To facilitate comparison the curves are normalized to the same value at a film thickness of 250 nm. Note that due to the weak optical nonlinearity of the film/glass interface the total SH signal is identical to the signal from the film. For other interfaces with a non-negligible χ_{int}, *e.g.* metal/polymer, the additional contribution from the interface superimposes on the film signal, according to Equation (5). This interference would alter the shape of the curves displayed in Figure 3.[17] The calculation illustrates that the variation of the SH signal as a function of film thickness can be drastically different depending on the molecular inclination angle, θ. However, there is a decrease in the variation of the thickness-dependent SH signal to changes of the tilt angle towards high values of θ. Up to about 40°, a pronounced sensitivity of the thickness-dependent SH signal to alterations of the tilt angle exists. For larger values this sensitivity is continuously decreasing. Depending on the linear optical properties of the film and the substrate, the sensitivity might be lost already above 60° or can extend up to 80°. It is obvious from the calculation that the SH signal does not increase quadratically with film thickness as one would expect at first glance from a coherent superposition of the contributions of

the molecules in the film. Maxima and minima occur which are caused by the field distribution of the fundamental and harmonic waves along the surface normal and which are determined by the linear optical properties of the film.

III. EXPERIMENTAL

Figure 4 shows schematically the experimental setup. The substrate was placed in a high-vacuum chamber (base pressure $< 1 \times 10^{-8}$ mbar). The dianhydride and the diamines were evaporated from two retractable Knudsen cells placed a few centimeters in front of the substrate. Before starting the deposition, the cells were warmed up to steady state conditions in a second vacuum chamber separated from the deposition chamber by a gate valve. A quartz crystal microbalance, which was placed in front of the cells instead of the substrate, served to determine the growth rate.

A standard optical setup, consisting of a Nd-YAG laser (10 ns pulses at 1064 nm, 10 Hz repetition rate), polarisers for the fundamental (1064 nm) and harmonic beams (532 nm), color glasses and a monochromator with a photomultiplier, was used. The second harmonic signal reflected from the substrate was measured. In all experiments, both the incident fundamental and the analysed second harmonic waves were polarised parallel to the plane of incidence (pp-polarisation). Growth rates were 10–12 Å/min. Polycrystalline gold films (100 nm) sputtered onto Si(100) with a 5 nm chromium interlayer served as substrates. PMDA (99%) and DAPS (95%) were purchased from

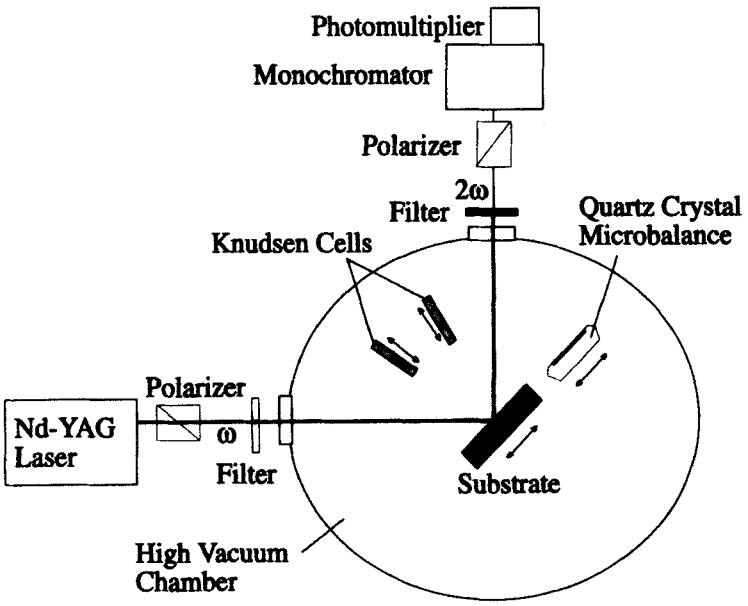

FIGURE 4 Scheme of the experimental setup.

Riedel-de Haen, ODA (> 95%) and benzidine (p.a.) from Fluka and used without further purification.

To ensure that the change of the SH signal during deposition is solely due to the increase in film thickness and not distorted by relaxation processes in the film, deposition was interrupted for 20 minutes in several experiments. No variation of the SH signal was observed during this period, and after the interruption the signal continued to change exactly as in experiments with continuous deposition. Blocking of the laser beam for some time was applied to check if heating of the film by absorption of laser light modifies the SH signal. No influence of the laser radiation was found. Furthermore, the formation of PACS was verified by grazing incidence IR measurements and X-ray photoelectron spectroscopy (XPS).

Theoretical curves were fitted to the experimental data based on the model described in Section II and a least-squares algorithm.[21] The linear optical constants served as input parameters and were determined by linear reflection and ellipsometric measurements. Fitting parameters were the tilt angle, θ, and the ratio of the SH activity of the film and the interface, χ_{zxx}/χ_{int}. In some experiments the film thickness calculated from the deposition time and the growth rate was scaled by a few percent. The scaling is given by the measurements in sp-polarisation. In this configuration, the maxima of the curves are determined by the thickness of the film and its linear optical properties but not by the orientation of the susceptibility, $\chi_{\xi\xi\xi}$.[17] Therefore, measurements in sp-polarisation provide a control of the accuracy of the QCM measurements.

IV. RESULTS

PMDA/DAPS

Figure 5 shows the SH signal recorded during the codeposition of PMDA and DAPS on gold. The thickness-dependent SH intensity has been normalised to the value of the clean substrate. Right at the beginning of the deposition, a distinct decrease of the second harmonic signal is observed. It indicates the formation of the interface. The flux of molecules was too high in this case to allow a time-resolved monitoring of this process. After the sudden drop, the SH signal continues to decrease slightly until a minimum is reached at around 12 nm. Subsequently, the signal rises with increasing film thickness and passes a maximum at about 200 nm.

The dotted and solid lines are fits based on the three-layer model outlined in Section II. In contrast to the curves of Figure 3, a contribution from the substrate/film interface has been taken into account. The fit represented by the solid line was obtained by using the whole range of the film thickness, *i.e.* 225 nm. A tilt angle of $\theta = 44°$ and a ratio of $\chi_{zxx}/\chi_{int} = 1.2 \times 10^{+4} e^{i137°}\ cm^{-1}$ is obtained. According to Equation (5), χ_{int} is the susceptibility right after the drop of the SH signal. Even though the experimental curve is described excellently over a range of more than 200 nm, a systematic deviation is readily identified for a film thickness below 20 nm. If the fit is based on the data points of the first 50 nm only, the dashed curve results. It describes the thin film region very well but deviates markedly for larger thickness. A smaller tilt angle of $\theta = 19°$ and a ratio of $\chi_{zxx}/\chi_{int} = 2.1 \times 10^{+4} e^{-i12°}\ cm^{-1}$ is obtained.

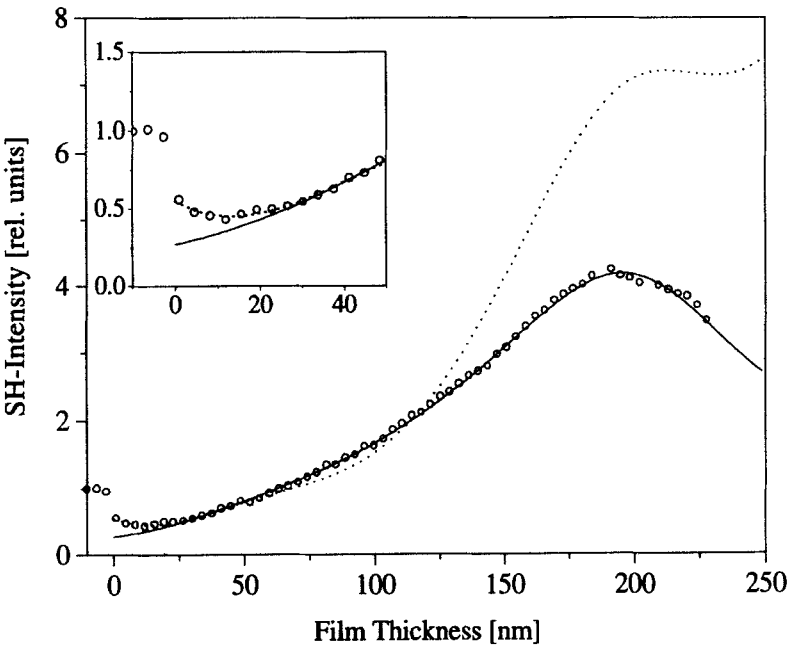

FIGURE 5 SH signal recorded during the growth of a polyamic acid film of pyromellitic dianhydride (PMDA) and 4,4'-diaminodiphenyl disulfide (DAPS) on gold. The thickness-dependent signal, which is normalised to the signal from the native substrate, was measured at 532 nm in pp-polarisation. The zero point of the x-axis marks the beginning of the deposition. The solid curve, which is based on the model described in the text, is a fit using the whole thickness range. The dashed curve represents a fit using the first 50 nm of film thickness only. The inset shows the first 50 nm on an expanded scale. The tilt angles for $\chi_{\zeta\zeta\zeta}$ obtained from the three-layer model are 44° (solid curve) and 19° (dashed curve). The ratio χ_{zxx}/χ_{int} is $1.2 \times 10^{+4} e^{i137°}\,cm^{-1}$ and $2.1 \times 10^{+4} e^{-i12°}\,cm^{-1}$, respectively.

PMDA/ODA

The thickness dependence of the SH signal for PMDA/ODA is depicted in Figure 6. In contrast to PMDA/DAPS, the sudden decrease of the SH signal during the initial stage of the deposition is lacking. The thin film region differs as well. With ODA, the SH signal stays constant up to a film thickness of about 15 nm. For thicker films, the SH signal behaves qualitatively the same as DAPS-PACS even though the ratio between the substrate signal and the maximum is about 4 times larger for PMDA/ODA than for PMDA/DAPS. This is explained partially by the fact that χ_{zxx} and χ_{int} are towards compensation ($\Delta\phi = 137°$) for PMDA/DAPS whereas a more constructive superposition ($\Delta\phi = 28°$) is present for PMDA/ODA.

Again, the dotted and solid lines are fits based on the three-layer model. A tilt angle of $\theta = 52°$ and a ratio of $\chi_{zxx}/\chi_{int} = 1.5 \times 10^{+4} e^{i128°}\,cm^{-1}$ is obtained using the whole thickness range (solid curve). Since PMDA/ODA does not show any interface reaction, χ_{int} equals the susceptibility of the clean substrate (χ_{sub}).

Even though the difference between the solid line of Figure 6 and the experimental data points is small within the first 20 nm of the film thickness a systematic deviation is

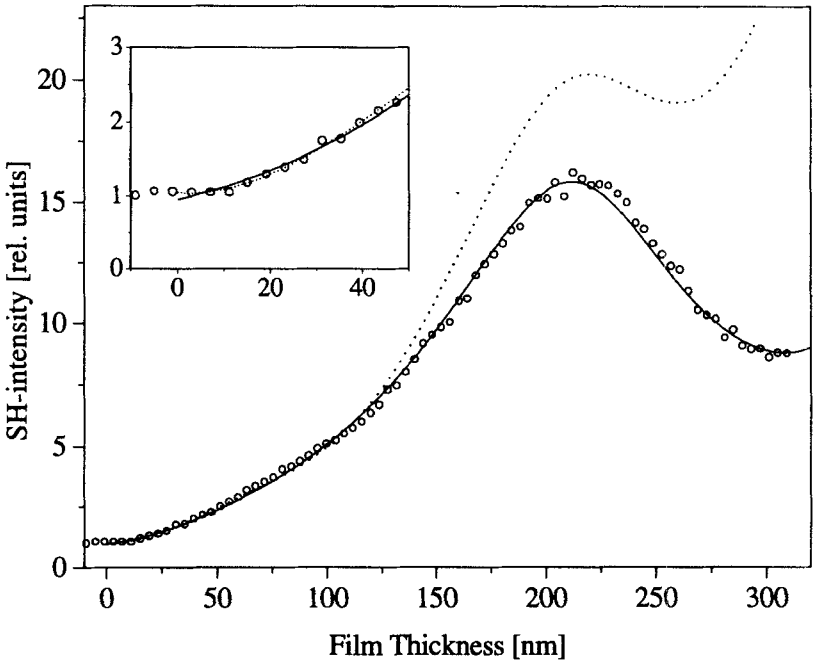

FIGURE 6 SH signal recorded during the growth of a polyamic acid film of pyromellitic dianhydride (PMDA) and 4,4'-oxydianiline (ODA) on gold. The thickness-dependent signal, which is normalised to the signal of the native substrate, was measured at 532 nm in pp-polarisation. The zero point of the x-axis marks the beginning of the deposition. The solid curve, which is based on the model described in the text, is a fit using the whole thickness range. The dashed curve represents a fit using the first 50 nm of film thickness only. The inset shows the first 50 nm on an expanded scale. The tilt angles for $\chi_{\xi\xi\xi}$ obtained from the three-layer model are 52° (solid curve) and 23° (dashed curve). The ratio χ_{zxx}/χ_{int} is $1.5 \times 10^{+4} e^{i28^\circ}\,cm^{-1}$ and $2 \times 10^{+4} e^{i6^\circ}\,cm^{-1}$, respectively.

present. Whereas the experiment yields a constant SH signal up to a thickness of 15 nm, the fit increases right from the beginning. Furthermore, the starting level of the fit is too low. In other experiments, this discrepancy was even more pronounced. In order to achieve a proper modelling of the initial stages of film growth, the range over which the data points are fitted had to be reduced. If the range is narrowed to the first 50 nm, an excellent agreement between experiment and simulation ia achieved in this range. The tilt angle of χ_{zxx} is reduced from 52° to 23° and a ratio of $\chi_{zxx}/\chi_{int} = 2 \times 10^{+4} e^{i6^\circ}\,cm^{-1}$ results.

PMDA/Benzidine

An example of a measurement is shown in Figure 7. As for PMDA/ODA, no interface reaction is identified. For the growing film, a behavior of the SH signal somewhat different from the other systems is observed. As seen from Figure 7, two main differences are obvious. The first one is the different shape of the SH curve and the second one is the small ratio of the maximum of the SH intensity to the signal of the bare substrate. In the case of PMDA/benzidine, a value of about 2.7 is obtained in

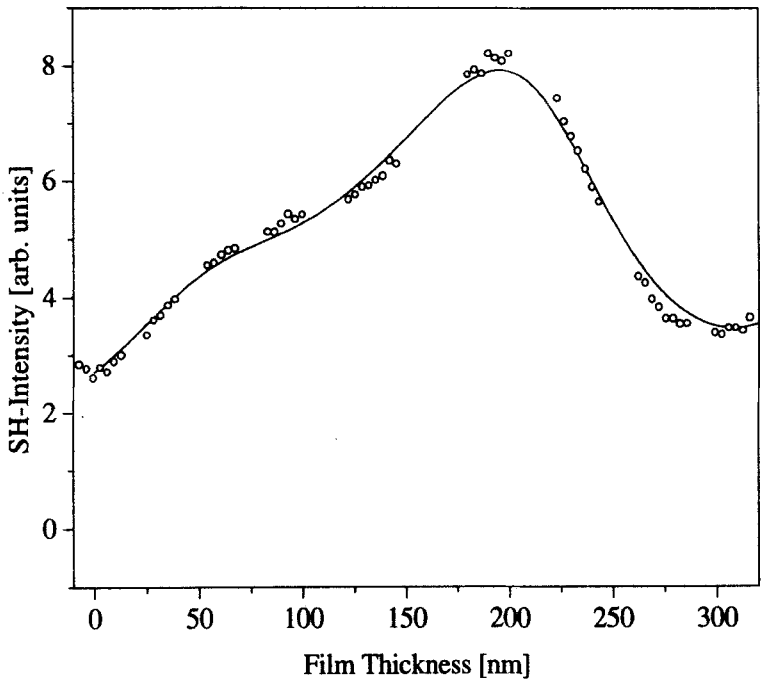

FIGURE 7 SH signal recorded during the growth of a polyamic acid film of pyromellitic dianhydride (PMDA) and benzidine on gold. The thickness-dependent signal, which is normalised to the signal of the native substrate, was measured at 532 nm in pp-polarisation. The zero point of the x-axis marks the beginning of the deposition. The solid curve is a fit based on the model described in the text. The tilt angle for $\chi_{\zeta\zeta\zeta}$ obtained from the three-layer model is 43°. The ratio χ_{zxx}/χ_{int} is $0.43 \times 10^{+4} e^{i9^\circ}$ cm^{-1}.

contrast to 17 for PMDA/ODA and 4 for PMDA/DAPS. For this measurement in pp-polarisation the data points are not continuous due to an alternating measurement in sp-polarisation. Since the polarisation dependence of the SH signal is beyond the scope of this paper the sp-polarised signal has been omitted. We refer to Reference 22 for a detailed discussion of this topic. A fit to the data over the whole thickness range yields $\theta = 43°$ and $\chi_{zxx}/\chi_{int} = 0.43 \times 10^{+4} e^{i9^\circ}$ cm^{-1}. The quality of the fits for PMDA/benzidine is generally lower compared with the other two systems. We ascribe this to fluctuations in the flux of benzidine since the vapor pressure of benzidine is more sensitive to temperature changes than DAPS or ODA. In principle, this problem could be overcome by using an excess of benzidine. In this case, the flux of PMDA would be rate limiting. However, an excess of dianhydride rather than diamine is favorable for good quality films[24] and in this case benzidine determines the growth rate.

V. DISCUSSION

The experimental data together with the fits based on the three-layer model suggest that it is possible to distinguish between three different stages of film growth. The first

one is the formation of the interface, *i.e.* the first layer, during the very initial stages of the deposition. The second one extends up to a film thickness of several ten nanometers followed by a third (wide) range with an orientation of $\chi_{\xi\xi\xi}$ different from the thin film region.

For PMDA/DAPS, the sudden drop of the signal results from the dissociative adsorption of DAPS on gold. As illustrated by Figure 8, an aminothiophenolate is formed on the gold substrate by breaking the S-S bond, in analogy to other disulfides.[23] As for thiols, the Au-S bond leads to a decrease of the nonlinear optical activity of the gold surface. The same behavior of the SH signal has been observed for DAPS and *n*-alkane thiol adsorption from solution and is used to monitor film formation at the liquid/solid interface *in situ* and in real time.[25] In those experiments, a time-resolved monitoring of the film formation was possible due to the low concentration of the molecules in the solution. In the present experiments, the flux of molecules was much higher and, therefore, only the final state after the interface formation is detected. The decrease of the SH signal by about 50% is the same as observed during the formation of dense films of *n*-alkane thiols. This means that the very first layer consists of DAPS. Consequently, the role of DAPS is twofold. First, it serves as the diamine component for the PACS film and, second, by dissociation as an adhesion link. In contrast, no interface reaction can be detected for PMDA/ODA and PMDA/benzidine. This is to be expected since none of the molecules reacts with gold.

The problems in fitting the experimental data depicted in Figures 5 and 6 with a single set of parameters imply that the film is not uniform over the whole thickness range. The fits describing the thin film region (dotted lines) exhibit a distinct deviation from the experimental data for the thick film region. For both PMDA/ODA and PMDA/DAPS, the calculated curves yield values which are too large. It seems that the contribution of χ_{zxx} decreases when going beyond the thin film region. This is substantiated by the ratios of the film and the interface susceptibilities obtained from the fits. However, a mere change of the orientation of the molecules cannot account for the two ranges. Assuming a constant value of $\chi_{\xi\xi\xi}$, the increase of θ from about 20° to above 40° also causes an increase of χ_{zxx} (see Eq. (7)), in contrast to the finding. Therefore, other effects must be responsible for the overall decrease of χ_{zxx}. One

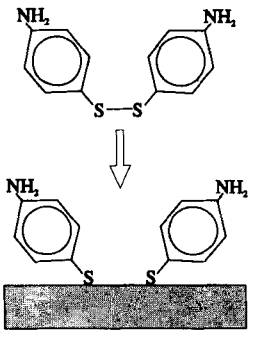

FIGURE 8 Dissociative adsorption of 4,4'-diaminodiphenyl disulfide (DAPS) on gold. The S-S bond breaks upon adsorption on gold and an aminothiophenolate is formed.

possibility is a broadening of the orientational distribution or, in other words, a more disordered structure of the film. This would mean an effectively lower density of the NLO-active units and, hence, a smaller value of χ_{zxx}. Another possibility is a conformational change of the molecular units, resulting in a variation of their electronic structure and, therefore, in an altered susceptibility of the molecule both in orientation and in magnitude. In any case, the fits depicted in Figures 5 and 6 suggest that after a range which can extend up to a thickness of several tens of nanometers a transition to a different structure takes place. Such structural transitions which can affect the mechanical properties of metal/polymer laminates are not uncommon. For example, in polyimide films prepared by spin coating, grazing incidence X-ray scattering experiments revealed a transition from the liquid-crystalline-like ordering of the bulk to an enhanced ordering of the interphase adjacent to the film-vacuum interface.[27]

Strictly speaking, however, the application of the three-layer model is not appropriate for films with a thickness beyond the point where the structural transition occurs. In general, a different structure is associated with different optical properties and, therefore, a description of the system by four layers is more appropriate. An extension of SHG to composites having more than three layers is possible using the transfer matrix formalism.[28] In the cases reported here, the differences in the optical properties between the different phases of the film are apparently very small and the treatment as a three-layer system results in minor deviations only. However, there are other cases where the three-layer model fails beyond the thin film region. For PMDA/ODA on silver, a rather abrupt change of the thickness-dependent SH signal is observed above 60 nm and the three-layer model is only able to describe the data up to this value.[17,22]

Another interesting issue to be addressed is the microscopic origin of the NLO signal of the film. PMDA is not expected to contribute significantly to the SH signal: in the case of formation of the polyamic acid *via* the para positions, the molecule remains centrosymmetric and, therefore, SH-inactive. In case of bonding in the meta positions, which takes place with about the same probability,[26] the inversion symmetry is lost. However, the groups in the 1,5 and the 2,4-positions are not that much different that a highly asymmetric molecule with high NLO activity could be formed. On the other hand, ODA and DAPS are highly asymmetric molecules due to their V-shaped structure and should be the source of the SH signal. This interpretation is corroborated by comparing the susceptibility ratios, χ_{zxx}/χ_{int}, for PACS containing DAPS or ODA, on the one hand, with PACS having benzidine as the diamine component, on the other hand. Since the phenyl rings are not bent towards each other in benzidine, the molecule is much less asymmetric than the other two diamines. This should result in a significantly smaller value for χ_{zxx}/χ_{int}. The experiment agrees completely with this interpretation.

In order to extract information on the orientation of the molecules, the microscopic susceptibilities have to be related to the tensor elements of the measured macroscopic susceptibility, χ_f. *A priori* there is no reason, of course, to assume that the molecular susceptibility has only one tensor component. Surprisingly, however, this assumption provides a very good description of the systems considered here. It is essential to mention that the need for two different sets of parameters for the thin and thick film regions is not due to the simplifying assumption of a one-dimensional susceptibility. Even with the choice of independent tensor elements, χ_{zzz}, χ_{zxx}, and χ_{xzx}, a correct

description of the whole thickness range is impossible with a single set of parameters. Nevertheless, even if the microscopic susceptibility has more than one tensor element, it can occur that due to the symmetry of the system the tensor appears pseudo one-dimensional.[22] This would explain the success of the simple model proposed in this work.

So far, structural transitions have been discussed only qualitatively. The model, however, yields quantitatively the tilt angle and the (relative) magnitudes of the film and interface susceptibilities. With these quantities one can, in principle, infer the orientation of the molecules in the film. However, the problem in determining the film structure from the SH signal is the relation between the molecular susceptibility and the geometry of the molecule. Only quantum chemical calculations can provide the connection between the nonlinear electronic properties of a molecule and its three-dimensional structure. The theoretical framework available today for such type of computation is not advanced enough to allow for a reliable calculation of the molecular NLO properties for arbitrary molecules and over a broad wavelength range. Therefore, the progress of the potential of SHG for the quantitative analysis of the structure of thin films is mainly determined by the pace with which the theoretical treatment can be improved.

CONCLUSION

The growth of thin films has been monitored *in situ* with optical second harmonic generation. The variation of the SH signal with film thickness is sensitively dependent on the substrate and the components of the film. Interface reactions and structural transitions of the growing film are reflected by the second harmonic signal. A model taking into account the optical properties of thin films reveals that the SH signal contains information about the elements of the susceptibility tensor. With a known relation between the susceptibility and the geometry of the molecule, SHG allows one to determine the angle of orientation and its changes during film growth.

Acknowledgements

We are grateful to H. Schwenk (Wacker Siltronic) and W. Schrepp (BASF) for providing us with the substrates and to T. Wagner (LOT) for technical support with respect to the ellipsometric measurements. This work was supported by the BMBF under grant no. 01BM206/3. Financial support of M.B. by the Deutsche Forschungsgemeinschaft is gratefully acknowledged.

References

1. G. L. Richmond, J. M. Robinson, V. L. Shannon, *Prog. Surf. Sci.*, **28**, 1 (1988).
2. Y. R. Shen, *Annu. Rev. Phys. Chem.*, **40**, 327 (1989).
3. Y. R. Shen, *Nature*, **337**, 519 (1989).
4. R. M. Corn, D. A. Higgins, *Chem. Rev.*, **94**, 107 (1994) and references therein.
5. F. Träger, A. Goldmann, Eds., *Surface Studies by Nonlinear Laser Spectroscopies* (Springer Verlag, Heidelberg, 1995).
6. A. Ulman, *Ultrathin Organic Films* (Academic Press, Boston, 1991).

7. B. Koopmans, A. Anema, H. T. Jonkman, G. A. Sawatzky, F. van der Woude, *Phys. Rev.*, **B48**, 2759 (1993); B. Koopmans, A. M. Janner, H. T. Jonkman, G. A. Sawatzky, F. van der Woude, *Phys. Rev. Lett.* **71**, 3569 (1993).
8. D. Wilk, D. Johannsmann, C. Stanners, Y. R. Shen, *Phys. Rev.*, **B51**, 10057 (1995).
9. M. S. Yeganeh. J. Qi, J. P. Culver, A. G. Yodh, M. C. Tamargo, *Phys. Rev.*, **B46**, 1603 (1992).
10. V. V. Balaniuk, V. F. Krasnov, S. L. Musher, A. M. Rubenchik, V. E. Ryabchenko, V. I. Prots, M. F. Stupak, S. G. Struts, *Opt. Commun.*, **79**, 333 (1990).
11. M. Grunze, M. Buck, in *Surface Science: Principles and Applications*, R. F. Howe, R. N. Lamb, K. Wandelt, Eds. (Springer Proc. in Phys. 73, Springer, Berlin, 1993), p. 67.
12. K. Kumagai, G. Mizutani, H. Tsukioka, T. Yamauchi, S. Ushioda, *Phys. Rev.*, **B48**, 14488 (1993).
13. J. Salem, F. O. Sequada, J. Duran, W. Y. Lee, R. M. Yang, *J. Vac. Sci. Technol.*, **A4**, 369 (1986).
14. K. L. Mittal, Ed, *Polyimides – Synthesis, Characterisation and Application*, Vols. 1 & 2 (Plenum Press, New York 1982/1984).
15. Y. R. Shen, *The Principles of Nonlinear Optics* (J. Wiley, New York, 1984).
16. N. Bloembergen, P. S. Pershan, *Phys. Rev.*, **128**, 606 (1962).
17. Ch. Dressler, PhD Thesis, Heidelberg, 1994.
18. M. Born, E. Wolf, *Principles of Optics* (Pergamon Press, Oxford, 1980).
19. E. T. Arakawa, M. W. Williams, J. C. Ashley, L. R. Painter, *J. Appl. Phys.* **52**, 3579 (1981).
20. W. G. Driscoll, W. Vaughan, Eds., *Handbook of Optics* (McGraw Hill Publ., New York, 1978).
21. W. H. Press, B. P. Flannery, S. A. Teukolsky, W. T. Vetterling, *Numerical Recipes in C* (Cambridge University Press, Cambridge, 1988).
22. M. Buck, Ch. Dressler, M. Grunze, F. Träger, in preparation.
23. L. H. Dubois, R. G. Nuzzo, *Annu. Rev. Phys. Chem.*, **43**, 437 (1992).
24. R. G. Pethe, C. M. Carlin, H. H. Patterson, W. N. Unertl, *J. Mater. Res.*, **8**, 3218 (1993).
25. M. Buck, F. Eisert, J. Fischer, M. Grunze, F. Träger, *J. Vac. Sci. Technol.*, A **10**, 926 (1992).
26. M. I. Bessonov, M. M. Koton, V. V. Kudryavtsev, L. A. Laius, *Polyimides: Thermally Stable Polymers* (Plenum Publ., New York, 1987).
27. B. J. Factor, T. P. Russell, M. F. Toney, *Phys. Rev.*, L ett. **66**, 1181 (1991).
28. D. S. Bethune, *J. Opt. Soc. Am.*, **B 6**, 910 (1989); D. S. Bethune, *J. Opt. Soc. Am.*, **B 8**, 367 (1991).